Submitted to Journal of Electroanalytical
Chemistry and Interfacial Electrochemistry

UCRL-20557 Rev.
Preprint c.2

UNSTEADY-STATE EFFECTS IN LIMITING CURRENT MEASUREMENTS

J. R. Selman and C. W. Tobias

June 1975

Prepared for the U. S. Energy Research and
Development Administration under Contract W-7405-ENG-48

TWO-WEEK LOAN COPY

This is a Library Circulating Copy
which may be borrowed for two weeks.
For a personal retention copy, call
Tech. Info. Division, ~~Ext. 5545~~

LAWRENCE BERKELEY LABORATORY
UNIVERSITY OF CALIFORNIA
BERKELEY

UCRL-20557 Rev.
c.2

DISCLAIMER

This document was prepared as an account of work sponsored by the United States Government. While this document is believed to contain correct information, neither the United States Government nor any agency thereof, nor the Regents of the University of California, nor any of their employees, makes any warranty, express or implied, or assumes any legal responsibility for the accuracy, completeness, or usefulness of any information, apparatus, product, or process disclosed, or represents that its use would not infringe privately owned rights. Reference herein to any specific commercial product, process, or service by its trade name, trademark, manufacturer, or otherwise, does not necessarily constitute or imply its endorsement, recommendation, or favoring by the United States Government or any agency thereof, or the Regents of the University of California. The views and opinions of authors expressed herein do not necessarily state or reflect those of the United States Government or any agency thereof or the Regents of the University of California.

UCRL-20557 Revised

UNSTEADY-STATE EFFECTS IN LIMITING CURRENT MEASUREMENTS

by

J. R. Selman* and C. W. Tobias

Inorganic Materials Research Division,
Lawrence Berkeley Laboratory, and
Department of Chemical Engineering;
University of California, Berkeley 94720

*Present address: Department of Chemical Engineering, Illinois Institute of Technology, Chicago, Ill. 60616

Introduction

Measurements of limiting currents have been widely adapted during the past 25 years for the study of mass transport conditions at solid-liquid interfaces. The relative simplicity of the experimental apparatus, and the facility with which a limiting current plateau may be determined lead to a widespread application of this technique, beyond the traditional boundaries of "electrochemistry".[1,2] Limiting current measurements allow the determination of mass transfer coefficients with a better accuracy than that offered by other methods available for this purpose.

This communication is concerned with the analysis of unsteady-state effects in the measurement of limiting currents. The response of transport processes to the driving force, the applied potential, requires careful consideration in the design of the experiment and in the interpretation of data.

The following methods have been commonly employed for reaching the limiting current:

1. Application of a single overpotential step which is sufficient to allow the limiting condition to be reached, but not large enough to allow a consecutive electrode process to occur.[3]
2. Stepwise increase of the current, or of the overpotential. Steps may be well defined (programmed) or may be applied in a more or less arbitrary fashion.[4,5,6]
3. Application of a current ramp or of a linear potential scan, with adjustable rate of increase of current, or of potential.[7,8,9]

4. In studies involving forced convection: application of a constant current and diminishing the intensity of convection (e.g., by reducing the rate of flow or the velocity of movement of the electrode) until limiting condition is reached.[10]

Each of these methods are supposed to allow the determination of the true steady state limiting current, which corresponds to a negligibly small concentration of reactant at the electrode surface when the concentration profile in the mass transfer boundary layer has reached the steady state.

The time elapsed from the closing of the electrolysis circuit to reaching the limiting condition should be sufficient to establish the steady state concentration profile. This time period will clearly depend on the method chosen for reaching the limiting current, and on the prevailing hydrodynamic conditions which influence the nature and extent of the boundary layer.

The main considerations which prompt investigators to reach the limiting current as rapidly as possible are as follows: a) When a small volume of electrolyte is used (e.g., in a non-flow system) the bulk concentration may undergo significant change during the experiment.[11] b) When the electrode reaction involves the deposition of a metal (e.g., copper) the surface progressively roughens as the deposit builds up, causing a gradual change of the surface area and of the character of the mass transfer boundary layer.[12] The effect of progressive surface roughening may be sufficiently severe to preclude obtaining a limiting plateau at all.

The development of steady state convective diffusion requires finite time. Because the concentration profile in forced convection is determined by the imposed velocity field* the estimation of the time required to establish steady state is relatively straightforward. Such is not the case when only the gravitational force acts on the fluid. Here the fluid motion results from the density gradient that develops as a consequence of depletion (or augmentation) of concentration of reacting species at the electrode. Development of the velocity field lags behind the development of the density gradient at the surface. Because the driving force depends on the concentration difference between bulk and interface, the mass transport process in dilute electrolytes requires longer time periods to reach steady state than in concentrated media. Prolonged electrolysis required in such cases can lead to bulk depletion and (in the case of metal deposition reaction) excessive surface roughening. Therefore, to obtain a steady state limiting current in the shortest possible time is generally a more critical problem in free convection studies.

Fenech[6] observed the dependence of apparent limiting currents on the method (i.e., stepwise or continuous) by which the limiting condition was reached. Hickman[13] employed a linear current ramp

---

*Although the concentration profile of the reacting species depends the current density, in the presence of large excess of supporting electrolyte, this will have only minor influence on the velocity field.

in an effort to devise a well defined, reproducible method for the execution of limiting current measurements. In the deposition of copper from stagnant acidified copper sulfate solutions onto a cathode facing downward, Hickman found that i_{AL}, the apparent limiting current (i.e., current at the transition time) decreases as $\frac{di}{dt}$ is reduced (fig. 1). As shown in fig. 2, when the orientation of the cathode is changed to face upward, thereby allowing free convection, the apparent limiting currents again decrease with decreasing $\frac{di}{dt}$. In this case, however, a steady state value of i_L was obtained when the time elapsed between starting the current and reaching the limiting condition

$$t = i_L \Big/ \frac{di}{dt} > 8 \text{ minutes} . \qquad (1)$$

Using linear increase of ΔE, the cell potential, Fenech[6] found that reproducible, steady state i_L could be obtained for copper deposition on horizontal electrodes facing upward when

$$t = 500\text{mv} \Big/ \frac{d(\Delta E)}{dt} > 3 \text{ min} . \qquad (2)$$

However, when the bulk concentration of $CuSO_4$ was below 0.01M, difficulties were encountered in obtaining reproducible limiting currents. As shown in fig. 3,instead of well defined plateaus, maxima and minima appeared in the i vs ΔE curves. The current maximum at 0.3 volt decreased when a lower scan rate was applied, but it didn't disappear. This "camel-back" type limiting current curve

may be explained by the long time required in dilute solutions for exceeding the Raleigh stability limit. The current maximum results from unsteady state diffusional transport, and when the transition time is reached the current begins to decline until the slowly developing convection eventually improves the transport of reacting ion to the surface. The current again ascends until the electrode potential reaches the value required for hydrogen evolution to begin. Unfortunately neither the current maximum, nor the minimum may be interpreted as corresponding to the true steady state limiting current, since throughout this time period the density profile near the electrode, hence the velocity field, is not fully developed.

Rather dramatic evidence of the effect of slowness of the development of convective patterns may be found in Böhm and Ibl's[14] study of transport by free convection between narrowly spaced electrodes. $Fe(CN)_6^{4+}$ was reduced on a nickel electrode which formed together with a parallel diaphragm a vertical slit open at both ends. Flow to and from a large reservoir of electrolyte resulted from the change in density in the gap. In small gaps the limiting current wouldn't reach steady state even after several hours. The use of copper deposition for the study of this model is clearly not suitable; the gradually increasing surface roughness makes it impossible to achieve steady state convective flow.

A comparison between times required to reach limiting current under free convection and under forced convection by either a current ramp or by potential scan is not possible because experimental data

and relevant theory are both lacking. However, some insight can be gained by examining the results available for a simpler boundary condition, namely for a concentration step at the electrode. These solutions were obtained for free convection at a vertical planar electrode and for forced convection between parallel plates (Lévêque - type mass transfer). Table I presents representative values of the time required to reach i_L for these two cases. The values for transient free convection at a vertical electrode were calculated from an approximate solution by Siegel,[15] in the dimensionless form:

$$\frac{Dt}{x^2} (Gr_x Sc)^{1/2} = 3 . \tag{3}$$

The time elapsed to reach a steady state concentration profile in Lévêque-type mass transfer (mass-transfer entrance regime in high-Sc fluids) was calculated from the solution by Soliman and Chambré:[16]

$$\frac{Dt}{x^2} \left(\frac{Sx^2}{D}\right)^{2/3} = 1.25 \tag{4}$$

for a 99% complete approach to the steady state. S is the transverse velocity gradient at the wall. For example in flow between parallel plates $S = 6u_{avg}/H$, where u_{avg} is the average linear velocity and H the distance between the plates.

As shown by eqs. (3) and (4), the time elapsed before local steady state is achieved depends on the distance along the mass-transfer surface in the streamwise direction, x . Furthermore, in slow forced

Table I. Time required to reach steady state limiting current (in seconds) in laminar free and forced convection along a planar electrode in a solution of 0.05M $CuSO_4$, 1.5M H_2SO_4 at 25°C. Current densities (in ma/cm^2) are bracketed.

Distance from leading edge (cm)	0.5	1	5	10	40
Free convection at vertical plate	42 (2.84)	60 (2.40)	133 (1.61)	189 (1.35)	377 (0.95)
Forced convection between parallel plates (1 cm distance)					
Re = 10	95 (1.31)	151 (1.04)	444 (0.61)	707 (0.48)	1777 (0.30)
100	21 (2.82)	33 (2.24)	96 (1.31)	151 (1.04)	382 (0.65)
1000	4.4 (6.08)	7.1 (4.83)	21 (2.82)	33 (2.24)	83 (1.41)
2000	2.8 (7.66)	4.4 (6.08)	13 (3.56)	21 (2.82)	52 (1.78)

laminar flow (Re < 100) transition times are comparable to those in laminar free convection.

The times listed in Table I are valid only for the response to a step in the reactant concentration at the electrode. Because in the step approach a current equal to the limiting current (or a sufficiently negative potential) is imposed already at $t = 0$, it is to be expected that the times necessary to generate steady-state limiting currents by a current ramp or by potential scan are longer than the simple transition times given by eq. (3) or eq. (4).

In the following results of two series of experiments are presented in which steady state limiting currents were generated by a current ramp and by potential scan. The minimum times required to reach limiting current by these two methods are then compared to those required when a current or potential step is applied instead. In experiments using potential scan, unlike in earlier work,[4,6] instead of the cell voltage, the cathode potential was controlled relative to an identical reference electrode.

For sake of convenience, the rotating disk was chosen as the experimental vehicle; here the mass flux is uniformally distributed over the electrode surface when limiting current is reached. To avoid complications arising from changes in the surface morphology during passage of current, reduction of ferric-cyanide was selected as the electrode reaction.

Experimental

A Wenking 61 RH potentiostat was used both in the potential scan and current ramp experiments; in the latter the potential drop over a fixed resistance was controlled.

Current and electrode potential were recorded by a Vidar 12289 Low-Level Data Logging System, consisting of a Vidar 510 Integrating Digital voltmeter, Vidar 12029 scanner, Vidar 625 Digital clock, Franklin 1040 High-Speed Printer, and Vidar 650-8 Coupler. The data in digital form were either printed out directly, or stored on magnetic tape and processed by computer. The highest scanning speed was 30 signals per second.

The rotating disks employed were of the design recommended by Riddiford, with an embedded nickel electrode of 0.4 cm diameter. Before each series of experiments, to obtain clean, stabilized surfaces, the disk and the nickel reference electrode were pre-treated by cathodic hydrogen evolution in 5% NaOH solution at a current density of 20 ma/cm^2 for 10 to 15 minutes.

The electrolyte was an equimolar solution of $K_3Fe(CN)_6$ and $K_4Fe(CN)_6$ prepared from reagent grade chemicals, with NaOH added as supporting electrolyte. The concentration of $K_3Fe(CN)_6$ was approximately 0.02M , that of NaOH 0.4M . The exact reactant concentrations and physical properties for the two series of measurements are given in Table II. Experiments were conducted at 25.0 ± 0.1°C .

Table II. Properties of electrolytes.

$$c_{K_3Fe(CN)_6} = c_{K_4Fe(CN)_6};\ c_{NaOH} = 0.4M$$

A. Current-ramp measurements:

$c_{Fe(CN)_6^{3-}} = 0.0184M$

$\rho = 1.022$ g/ml

$\mu = 0.985$ cp

$D = 7.88 \times 10^{-6}$ cm^2/sec

B. Potential-scan measurements:

$c_{Fe(CN)_6^{3-}} = 0.0143M$

$\rho = 1.021$ g/ml

$\mu = 0.984$ cp

$D = 7.89 \times 10^{-6}$ cm^{2}sec

Results

A. Current ramps

A series of current ramps were applied at two different rotation speeds (115 and 491 rpm), with di/dt ranging from 0.005 to 12 ma/cm^{2}sec . Figure 4 illustrates the curves obtained. The limiting current plateau gradually approaches horizontal inflection as di/dt is increased. The apparent limiting current was taken to be the value at the inflection point; this was located at approximately -900 mv overpotential except at the highest rates of increase, where it tended to shift to higher potentials (up to -1.1 volt).

Table III allows a comparison of results obtained at different speeds of rotation. In unsteady state mass transfer at a rotating disk the time may be rendered dimensionless by combining it with the diffusivity and the mass transfer boundary layer thickness, δ . This yields:

$$\tau = \omega t Sc^{-1/3} . \tag{5a}$$

If we now insert in eq. 5a the time in which a current ramp reaches the current level corresponding to steady state limiting current, we can write:

$$\tau' = \frac{i_L \omega Sc^{-1/3}}{di/dt} . \tag{5b}$$

Figure 5 shows the results in a double-logarithmic plot of apparent limiting currents relative to the steady-state value, against the dimensionless time τ' . At short times the apparent limiting current appears to tend toward a cube root dependence on time.

The results may now be compared with the time in which the steady-state concentration is established following a current <u>step</u> at the rotating disk. According to a solution by Hale,[17] the stationary concentration is established to within 1% in a time-period

$$\tau'_S = \omega t \; Sc^{-1/3} = 5.46.^{*} \tag{6}$$

This time is indicated as τ_{step} in Fig. 5.

The minimum time to obtain steady-state limiting currents by means of a current ramp, $\tau'_L \simeq 60$, is apparently an order of magnitude larger than τ_{step} .

---

*Superscript ' is used to denote current control while '' refers to potential control. Subscript L is used for time required to establish steady state.

Table III. Apparent limiting current values obtained by current ramps.

115 rpm			491 rpm		
$\frac{di}{dt} \times 10^{-3}$ (ma/cm^{2}sec)	i_{AL} (ma/cm^2)	$\tau' = \frac{i_L \omega Sc^{-1/3}}{di/dt}$ dimensionless	$\frac{di}{dt} \times 10^{3}$ (ma/cm^{2}sec)	i_{AL} (ma/cm^2)	$\tau' = \frac{i_L \omega Sc^{-1/3}}{di/dt}$ dimensionless
5.03	3.18	723	130	5.19	192
5.43	3.16	670	133	5.19	188
10.3	3.23	353	258	5.20	96.7
10.4	3.23	350	260	5.24	95.9
21.7	3.23	168	414	5.31	60.2
81.6	3.37	44.6	421	5.31	59.3
163	3.56	22.3	835	5.53	29.9
172	3.38	21.1	857	5.48	29.1
261	3.60	13.9	1700	5.96	14.7
266	3.62	13.7	1760	5.71	14.2
494	4.00	7.36	3370	6.35	7.41
506	4.03	7.19	3400	6.29	7.34
1063	4.57	3.42	6660	7.30	3.75
1150	4.62	3.16	6700	7.42	3.73
2040	5.23	1.78	11620	8.34	2.15
2140	5.35	1.70	11620	8.42	2.15
4360	6.42	0.834			
4680	6.48	0.777			
6975	7.66	0.522			
7040	7.62	0.517			

B. Linear potential scan

A series of potential scans were made at 490 rpm, ranging from $d\eta/dt = -5$ mv/sec to -2 v/sec . Figure 6 illustrates the i vs η curves thus obtained. In the limiting-current region current fluctuations (±1%) with a frequency somewhat higher than 1 sec^{-1} were observed; these appear to be characteristic for potential control in that region. The limiting-current value was determined by averaging over the plateau which extended here between -400 and -800 mv.

At higher scan rates the plateau was reached at more positive values (-200 mv); this was apparently due to an incipient current maximum at approximately -100 mv. At the highest scan rates the maximum could be clearly recognized (Fig. 6,c and d). When a current peak occurred, the following current plateau was higher than the steady-state limiting current.

Table IV lists the peak and plateau currents, and the potential scan rates. The scan times may be expressed in the dimensionless form

$$\tau'' = \omega t \, Sc^{-1/3} = \frac{\omega \, Sc^{-1/3}}{d\phi/dt} = \frac{\omega \, Sc^{-1/3} RT}{(d\eta/dt)nF} \, . \qquad (7)$$

Note that t in eq. (7) is the time in which the scan reaches a potential $-RT/nF$ (or -25.6 mv at 25°C for the reaction used in this work)and that the time to reach a potential of -400 mv, corresponding to the limiting current, is approximately 15 times greater.

Table IV. Apparent limiting current values obtained by linear potential decrease. (490 rpm).

$d\eta/dt$ (mv/sec)	i_{AL} (ma/cm^2)	i_{max} (ma/cm^2)	$\tau'' = \frac{\omega\ Sc^{-1/3}}{di/dt}$ dimensionless
4.55	4.76	-	26.50
8.77	4.78	-	13.75
17.6	4.79	-	6.85
27.9	4.79	-	4.33
27.9	4.80	-	4.33
54.7	4.84	-	2.21
114	4.89	5.16	1.05
221	5.01	5.95	0.546
433	5.14	8.30	0.279
436	5.13	8.28	0.277
633	5.46	9.48	0.919
920	5.70	11.05	0.131
2165	8.06	16.5	0.0557
2097	8.06	16.5	0.0575

Figure 7 shows in a double-logarithmic plot the apparent limiting currents (plateaus) and peak currents, relative to the steady-state limiting currents, against the dimensionless time (eq. 7). At short times the apparent limiting currents seem to depend inversely on the square root of the dimensionless time.

The time of transition to the steady-state limiting current by a potential scan may now be compared with the time in which the steady-state flux is established following a concentration step at the rotating-disk electrode. Solutions for the concentration-step transient were given by Olander[18] and by Filinovskii and Kiryanov.[19] A numerical solution valid for high-Sc mass transfer has been obtained[1] which shows that the stationary flux at the electrode is established to within 1% in a time-period

$$\tau''_S = \omega t \, Sc^{-1/3} = 2.05 \; . \qquad (8)$$

This time is indicated as τ_{step} in Fig. 7.

Taking the value of current at $-300 > \eta > -400$ mv , the minimum scan period to reach steady state limiting currents is $\tau'' \simeq 20$. As in the case of current ramps, this is an order of magnitude larger than τ''_S , the time required to reach steady state following a potential <u>step</u>. Thus, compared to the approach to steady state limiting current by a current ramp, the potential scan technique is approximately three times faster.

Discussion

The results of both types of unsteady-state limiting-current measurements may be interpreted in terms of a pure-diffusion model which is valid at the limit of high rates of current or potential increase.

Near the disk surface the convection velocity toward the disk is

$$u_y = -\alpha y^2 \omega^{3/2} \nu^{-1/2} \tag{9}$$

where $\alpha = 0.51023$. The convective term in the equation of convective diffusion is very small if

$$\frac{u_y y}{D} << 1 \rightarrow y << \left(\frac{\nu}{\omega}\right)^{1/2} Sc^{-1/3} \tag{10}$$

i.e., an order of magnitude smaller than the steady-state diffusion layer.

In very fast transients the limiting current condition $(c \approx 0)$, or a current maximum, is reached before the diffusion-layer has grown enough to make convective transport important. This is evident in particular from the potential-scan experiments, where the pure-diffusion phase distinctly precedes the convective-diffusion phase if the scan rate is fast enough.

In the following the pure-diffusion model is first applied to a deposition reaction. The results are then reconsidered for a redox reaction.

A. Current-ramp experiments

The response of the concentration at the electrode, c_o, to a linearly increasing cathodic flux:

$$N = -D\left(\frac{\partial c}{\partial y}\right)_o = -c_b st \tag{11}$$

is[20]:

$$\frac{c_o - c_b}{c_b} = \frac{-4st^{3/2}}{3(\pi D)^{1/2}}, \tag{12}$$

where

$$s = \frac{|dN/dt|}{c_b} \tag{13}$$

and c_b is the bulk concentration.

Zero concentration at the electrode is reached in a time

$$t = \left(\frac{9\pi D}{16\ s^2}\right)^{1/3}, \tag{14}$$

and the flux will be $1.209\ c_b(sD)^{1/3}$. Therefore, at high current increase rates the apparent limiting current is proportional to $(di/dt)^{1/3}$. In terms of the dimensionless variables of Figure 7:

$$i_{AL}/i_L = 1.662\left(\frac{i_L \omega\ Sc^{-1/3}}{di/dt}\right)^{-1/3}. \tag{15}$$

This equation is shown as a solid line in Figure 7. Although the experimental values deviate from eq. (15) they tend toward the theoretical line at higher values of di/dt .

The deviation from eq. (15) cannot be ascribed to the fact that a redox reaction is involved. Since the flux is controlled, eqs. (11-14) are valid for the oxidized species, i.e., the ferricyanide ion (ox) . The accumulation of the reduced species (red) at the cathode will also be according to eq. (12), but with D_{red} substituted for D_{ox} , and s_{red} equal to s_{ox} in an equimolar solution. The concentration overpotential is then

$$\eta = \frac{RT}{F} \ln \left\{ \frac{1 - A^{1/2} t^{3/2}}{1 + kA^{1/2} t^{3/2}} \right\} \tag{16}$$

where

$$A = \left(\frac{16\ s_{ox}^2}{9\pi D_{ox}} \right)^{1/3} , \tag{17}$$

and

$$k = \left(c_{ox,b} D_{ox}^{1/2} \right) / \left(c_{red,b} D_{red}^{1/2} \right) . \tag{18}$$

For the experimental solutions $k \simeq 1.1$.[1] From eq. (16) it is clear that the time passed until the potential is sufficiently negative for hydrogen ion reduction will be less than the theoretical time (eq. 14). The limiting current then will be less than predicted by

eq. (15). A similar reasoning shows that charge transfer overpotential, if significant, would lead to a lower limiting current. It is also unlikely that capacitive effects are important since for this reaction the surface overpotential is negligible compared to the concentration overpotential.

The most probable cause of the positive deviations from the pure-diffusion asymptote is the contribution of convective supply of reactant, even at high rates of current increase. (See Discussion, Section C.)

It is interesting to compare the results of Hickman[12] (Fig. 1) with eq. (14). The proportionality between t and $s^{2/3}$ is very satisfactory (Fig. 8). The diffusivity of Cu^{++} derived from the slope is $D = 4.73 \times 10^{-6}$ cm^2/sec, in good agreement with rotating-disk effective diffusivities.[1,21] Note that the data point for the lowest di/dt deviates most from the least-squares slope. This is probably caused by secondary convection at the edges of the embedded electrode.

B. Potential scan experiments

The response of the flux at the electrode, N, to a concentration step, $c_b - c_o$, is well-known:

$$N = -D\left(\frac{\partial c}{\partial y}\right)_o = -(c_b - c_o)\sqrt{\frac{D}{\pi t}} . \qquad (19)$$

If the surface overpotential and ohmic potential drop are negligible, the boundary condition for a linear potential scan

$$a = \frac{d\phi}{dt} = \frac{nF|d\eta/dt|}{RT} \tag{20}$$

is

$$t > 0 \ , \ y = 0 \ , \ c_o = c_b e^{\pm at} \tag{21}$$

and, by application of the superposition theorem, for a negative scan:

$$N = -c_b \sqrt{aD} \frac{2}{\sqrt{\pi}} P(\sqrt{at}) \tag{22}$$

where the function

$$P(y) = e^{-y^2} \int_0^y e^{\lambda^2} d\lambda \tag{23}$$

has a maximum $P(0.92414) = 0.54104$.[22]

The current maximum in potential scanning accordingly should depend on $(aD)^{1/2}$, i.e., on $(d\eta/dt)^{1/2}$:

$$i_{max} = -0.610503 \ c_b nF\sqrt{aD} \ , \tag{24}$$

or in terms of the dimensionless variables of Figure 7:

$$i_{max}/i_L = 0.9838\left(\frac{\omega\ Sc^{-1/3}}{d\phi/dt}\right)^{-1/2} . \tag{25}$$

The potential at the peak should be independent of $d\eta/dt$:

$$\eta_{max} = -0.8540\ RT . \tag{26}$$

It is to be noted that the peak current is not a limiting current in the usual sense, because $c_o = 0.426\ c_b$.

Since a redox reaction is involved, one should account for the contribution of the product ion (reduced species) to the overpotential. The accumulation of the product ion tends to decrease the potential to more negative values; when the potential is controlled, the result is a lowering of the current. The effect will be negligible in solutions with a small ratio of reactant (ox) to product (red) ion bulk concentration; in that case the conversion rate at the cathode is too small to cause a large shift of the potential with respect to the equilibrium potential. The effect will be large in solutions with an excess of reactant (ox) ion; a mathematical solution is available for this case (Sevcik-Randles equation).

In the present case of an equimolar solution no simplifications are possible. Consequently, a numerical solution had to be obtained using the characteristic diffusion parameter

$$k = \left(\frac{c_{ox,b}}{c_{red,b}}\right)\left(\frac{D_{ox}}{D_{red}}\right)^{1/2} . \tag{27}$$

For equimolar ferricyanide-ferrocyanide solutions $k \simeq 1.1$. The details of the numerical solution, which employed a procedure given by Acrivos and Chambré,[23] are given elsewhere.[1]

Figure 9 shows the current, expressed in dimensionless form:

$$I = -\frac{i}{c_{ox,b}nF}\left(\frac{\pi}{aD_{ox}}\right)^{1/2} , \tag{28}$$

against the logarithm of the dimensionless potential $\phi = -\eta nF/(RT)$. As a check on the accuracy of the solution, the parameter k was varied from 10^{-3} to 10^{+5} by decades. Below $k = 10^{-3}$ the current maximum has the value given by eq. (24), as in a deposition reaction, and its potential is given by eq. (26). At high values of k , i.e., for potentials much more positive than the standard redox potential, the current maximum has the value given by the Sevcik-Randles equation

$$i_{max} = 0.4463\ c_{ox,b}nF\sqrt{aD_{ox}} , \tag{29}$$

where the constant agrees to three significant figures with that computed by Nicholson and Shain.[24] The peak potentials become dependent on k shifting by $-\ln 10$ for every decade increase of k .

For the equimolar solution $(k = 1.1)$, the current maximum:

$$i_{max} = 0.52738\ c_b nF\sqrt{aD_{ox}} , \tag{30}$$

or

$$i_{max}/i_L = 0.84995\left(\frac{\omega\ Sc_{ox}^{-1/3}}{d\phi/dt}\right)^{-1/2} \quad . \tag{31}$$

The peak potential is $\phi = 1.6$, or $\eta = -41.1$ mv at 25°C.

Figure 7 shows that, for fast scans, eq. (30) predicts i_{max} reasonably well.

Girina, Filinovskii and Feoktistov[25] measured current maxima for reduction of Tl^+ at copper amalgam by potential scanning at a rotating disk electrode. They found good agreement with eq. (29), which is the appropriate equation for this reaction. As expected, the minimum scan period to reach a steady-state limiting current was accordingly shorter; the reported value corresponds to $\tau_L'' = 14$.

In the present work, the experimental peak potentials were larger than predicted, ranging from -65 to -190 mv, and increased with the scan rate. The ohmic drop included in the measured overpotential is probably responsible for this shift. At the highest peak currents the ohmic drop was estimated to be 35 mv. It is not unlikely that the inclusion of ohmic drop in the controlled potential leads to a shift of the peak potentials as large as those found experimentally. In view of the good agreement between predicted and observed current values this was not explored by further computations.

C. Minimum time to reach steady-state limiting current

The minimum time necessary to obtain a steady-state limiting current by means of a potential scan is appreciably shorter than the time needed in a current ramp ($\tau_L'' = 20$ vs $\tau_L' = 60$) . The ratio of

the minimum times is practically the same as the ratio of the times elapsed to steady state following a concentration or current step ($\tau''_S = 2.05$ vs $\tau'_S = 5.46$) . In both cases the difference between the two transients is caused by the relatively rapid depletion of the solution nearest the electrode if the potential is controlled, compared to a more gradual depletion, extending farther into the solution, when the current is controlled.

Under potential control the final adjustment of the concentration profile to steady state occurs mainly at a distance from the electrode, where the convective supply of reactant is ample. Under current control this final adjustment takes place close to the electrode where the convection is less effective. Consequently, to avoid "overshooting" the limiting current, a longer approach time is needed.

It is interesting in this connection to compare the current-time relationships for a potential scan and a current ramp, both leading to the steady-state limiting current in minimum time (Fig. 10). If the potential-scan response is approximated as an instantaneous step to the limiting current, the amount of reactant removed during the current ramp is 1.5 times that removed by the potential scan. This is another illustration of the greater effect of convection during current-ramps than during potential-scans.

Figure 10 also illustrates that a potential scan establishes a near-limiting current very rapidly compared to a current ramp. In deposition reactions where a rough, powdery deposit develops near the limiting current,[12] the shorter transition to the steady-state

limiting current may therefore be a questionable advantage of the potential-scan approach.

Conclusions

1. The minimum time to establish the steady-state limiting current at a rotating disk electrode was found to be $20\ Sc^{1/3}/\omega$ (seconds) in potential scanning, and $60\ Sc^{1/3}/\omega$ (seconds) for current ramps.

2. These minimum times are each an order of magnitude larger than those required to achieve steady-state following, respectively, a concentration step or a current step at a rotating disk electrode. The steady-state limiting current in free convection at horizontal electrodes is also reached neatly 3 times more rapidly by linear potential increase than by a current ramp.

3. As derived from consideration of convection-free diffusion, apparent limiting currents generated by high rate current ramps approach a dependence on $\left(\frac{di}{dt}\right)^{-1/3}$. The i_{AL} resulting from fast potential scans tend toward a dependence on $\left(\frac{d\eta}{dt}\right)^{-1/2}$, and the current maxima may be accurately predicted by considering the effect of unsteady state diffusion.

Summary

In the measurement of limiting currents, unless the approach to the mass transfer limiting conditions by a current ramp or by potential scan is sufficiently slow, the apparent limiting currents

obtained are higher than those corresponding to steady state transport.

A review of experimental results on limiting currents in free convection at horizontal electrodes indicates that steady state transport may be achieved nearly three times faster by potential scan than by a current ramp. Examination of limiting current data obtained on a rotating disk reveals that this is also the case in laminar forced convection.

An unsteady state diffusion model allows the prediction of the maximum current obtained in fast potential scanning. Criteria are established for estimating the time required for reaching steady state transport conditions when a current ramp or potential scan is used for the approach to limiting current.

Acknowledgement

This work was supported by the U. S. Energy Research Development Agency.

Symbols

a	normalized potential scan rate [sec^{-1}]
c	concentration [mole cm^{-3}]
D	diffusivity [$cm^2 sec^{-1}$]
ΔE	applied cell voltage [v]
F	Faraday's constant = 96501 C
H	distance between electrode plates in forced convection [cm]
i	current density [amp cm^{-2}]
i_{AL}	apparent (unsteady state) limiting current density [amp cm^{-2}]
i_L	steady-state limiting current density [amp cm^{-2}]
I	dimensionless current density, eq. (28)
k	redox diffusion parameter, eq. (27)
n	number of electrons transferred in reaction
N	mole flux [mole $cm^{-2} sec^{-1}$]
R	gas constant (8.3143 J/mole°K)
s	molar flux increase rate, eq. (11)
S	transverse velocity gradient at electrode [sec^{-1}]
t	time [sec]
T	temperature [°K]
u	velocity [cm sec^{-1}]
x	distance in direction of flow from leading edge of electrode [cm]
y	distance perpendicular to electrode [cm]

Greek Symbols

η overpotential [v]

μ viscosity [g $cm^{-1}sec^{-1}$]

ν kinematic viscosity [cm^2sec^{-1}]

ρ density [g cm^{-3}]

τ dimensionless time, eq. (5a)

τ' dimensionless time for current ramp, eq. (5b)

τ'' dimensionless time for potential scan, eq. (7)

τ'_L dimensionless time in which i_L is reached by current ramp

τ''_L dimensionless time in which i_L is reached by potential scan

τ'_S dimensionless time in which i_L is reached by current step

τ''_S dimensionless time in which i_L is reached by potential step

ϕ dimensionless overpotential ($\eta nF/RT$)

ω rotation rate [rad sec^{-1}]

Dimensionless Parameters

Gr_x Grashof number $g\Delta\rho x^3\rho^{-1}\nu^{-2}$

Re Reynolds number $2uH\nu^{-1}$

Sc Schmidt number νD^{-1}

Subscripts

b in the bulk

o at the electrode

max at the current maximum (potential scan)

ox pertaining to oxidized species

red pertaining to reduced species

References

1. J. R. Selman, "Measurement and Interpretation of Limiting Currents," Ph.D. Thesis, University of California, Berkeley, 1971, UCRL-20557.
2. T. Mizushina, Adv. Heat Transfer, vol. 7, 1971, p. 87.
3. U. Böhm, N. Ibl, and A. M. Frei, Electrochimica Acta, 11, 421 (1966).
4. C. R. Wilke, M. Eisenberg, and C. W. Tobias, J. Electrochemical Soc., 100, 513 (1953).
5. R. Dobry and R. K. Finn, Ind. Eng. Chem. 48, 1540 (1956).
6. E. J. Fenech, "Ionic Mass Transfer by Free Convection to Horizontal Electrodes," Ph.D. Thesis, University of California, Berkeley, 1960, UCRL-9079.
7. E. J. Fenech and C. W. Tobias, Electrochimica Acta, 2, 311 (1960).
8. Ch. W. Tobias and R. G. Hickman, Z. Physikal. Chemie (L), 229, 145 (1956).
9. C. A. Emery and R. E. Hintermann, Electrochimica Acta, 13, 127 (1968).
10. L. Hsueh and J. Newman, Electrochimica Acta, 12, 429 (1967).
11. C. W. Tobias and A. J. L. P. M. Böeffard, Ext. Abstr. 17th Mtg. C.I.T.C.E., Tokyo, 1966, pp. 23-24.
12. N. Ibl and K. Schadegg, J. Electrochemical Soc., 114, 54 (1967).
13. R. G. Hickman, "The Effect of Buoyancy Forces on Forced Convection Ionic Mass Transfer at Horizontal Planar Electrodes," Ph.D. Thesis, University of California, Berkeley, 1963.

14. U. Böhm and N. Ibl, Electrochimica Acta, 13, 891 (1968).

15. R. Siegel, Trans. Am. Soc. Mech. Eng., 80, 347 (1958).

16. M. Soliman and P. L. Chambré, Int. J. Heat Mass Transfer, 10, 169 (1967).

17. J. M. Hale, J. Electroanal. Chem., 6, 87 (1963).

18. D. R. Olander, Int. J. Heat Mass Transfer, 5, 825 (1962).

19. V. Yu. Filinovskii and V. Kir'yanov, Dokl. A. N. SSSR, 156, 1412 (1964) [Engl. 650 (1964)].

20. H. S. Carslaw and J. C. Jaeger, Conduction of Heat in Solids, 2nd ed., Oxford, 1959, p. 77.

21. L. Hsueh, "Diffusion and Migration in Electrochemical Systems," Ph.D. Thesis, University of California, Berkeley, 1968, UCRL-18597.

22. M. Abramowitz and I. A. Stegun, Handbook of Mathematical Functions, N.B.S., Washington, 1964, p. 319.

23. A. Acrivos and P. L. Chambré, Ind. Eng. Chem., 49, 1025 (1957).

24. R. S. Nicholson and I. Shain, Anal. Chem., 36, 706 (1964).

25. G. P. Girina, V. Yu. Filinovskii, and L. G. Floktistov, Elektrokhimiya, 3, 941 (1967) [Soviet Electrochemistry, 3, 831 (1967)].

Figure Captions

Figure 1. Apparent limiting currents on a horizontal electrode facing downward as a function of rate of linear increase of applied current. (From ref. 13.)

Figure 2. Apparent limiting currents on a horizontal electrode facing upward as a function of rate of linear increase of applied current. (From ref. 13.)

Figure 3. "Camel back" limiting current curve obtained by linear increase of applied cell potential. Slow development of free convection is a consequence of the low concentration of the reacting ionic species (6,7).

Figure 4. Apparent limiting currents generated by current ramps at a rotating disk electrode. Steady state $i_L = 3.18$ ma/cm^2.

Figure 5. Logarithmic plot of dimensionless apparent limiting current against dimensionless current increase rate. i_L = steady-state limiting current, i_{AL} = apparent limiting current [i.e., current density at the unsteady state transition time].

Figure 6. Apparent limiting current curves generated by means of potential scans at a rotating disk electrode $i_L = 4.79$ ma/cm^2.

Figure 7. Logarithmic plot of peak currents and apparent limiting currents against dimensionless potential scan rate. i_L = steady-state limiting current.

Figure 8. Interpretation of the data of Fig. 1 in terms of unsteady-state diffusion (eq. 14).

Figure 9. Current response to potential scanning for a redox reaction. $k = (c_{ox,b}/c_{red,b})(D_{ox}/D_{red})^{1/2}$. Dimensionless current, $I = -\frac{i}{c_{ox,b}nF}\frac{\pi}{aD_{ox}}^{1/2}$.

Figure 10. Comparison of current vs time during transition to the limiting current in minimum time by current ramp and by potential scan.

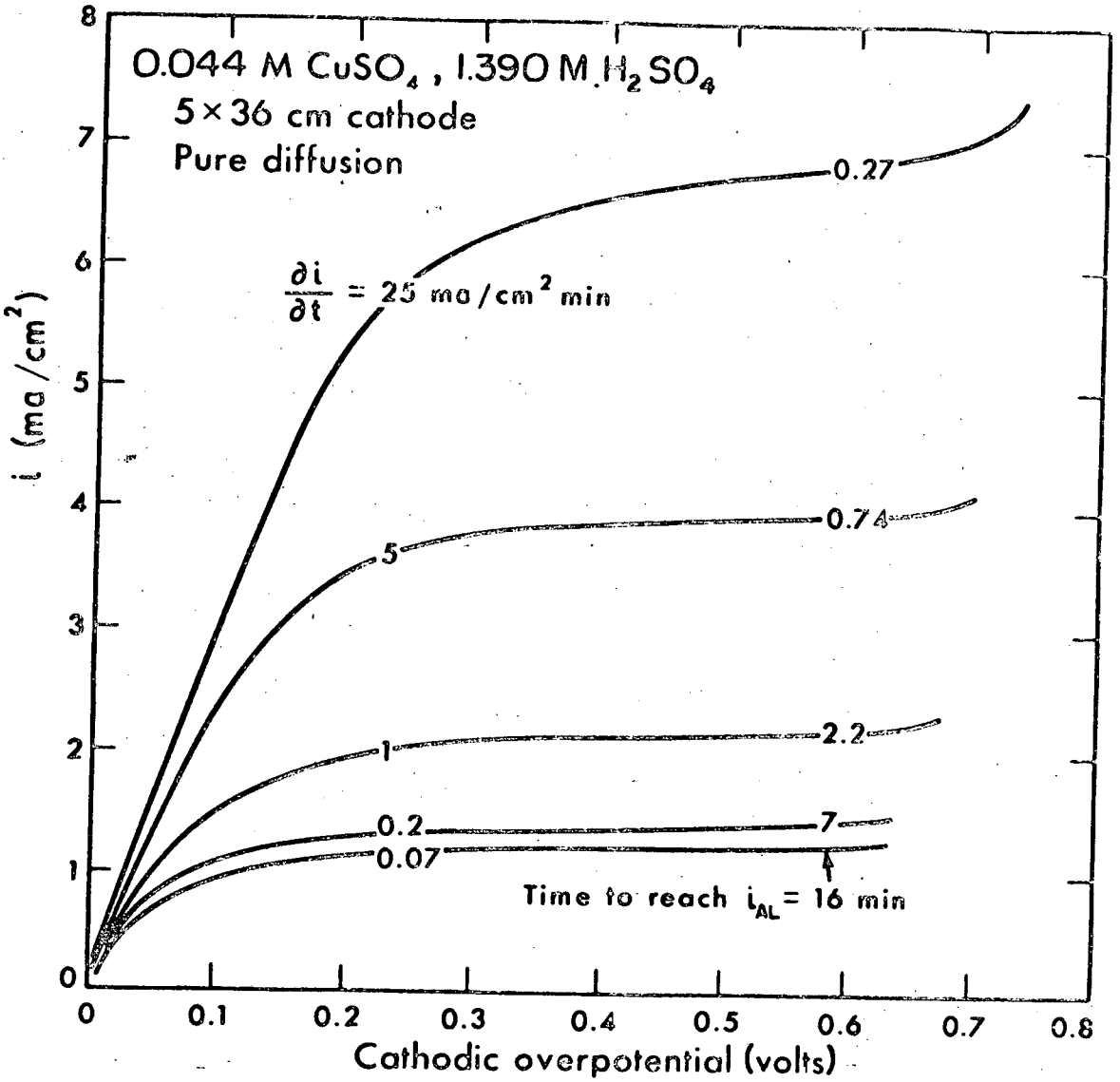

MUB 12040 A

Figure 1

Selman - Tobias

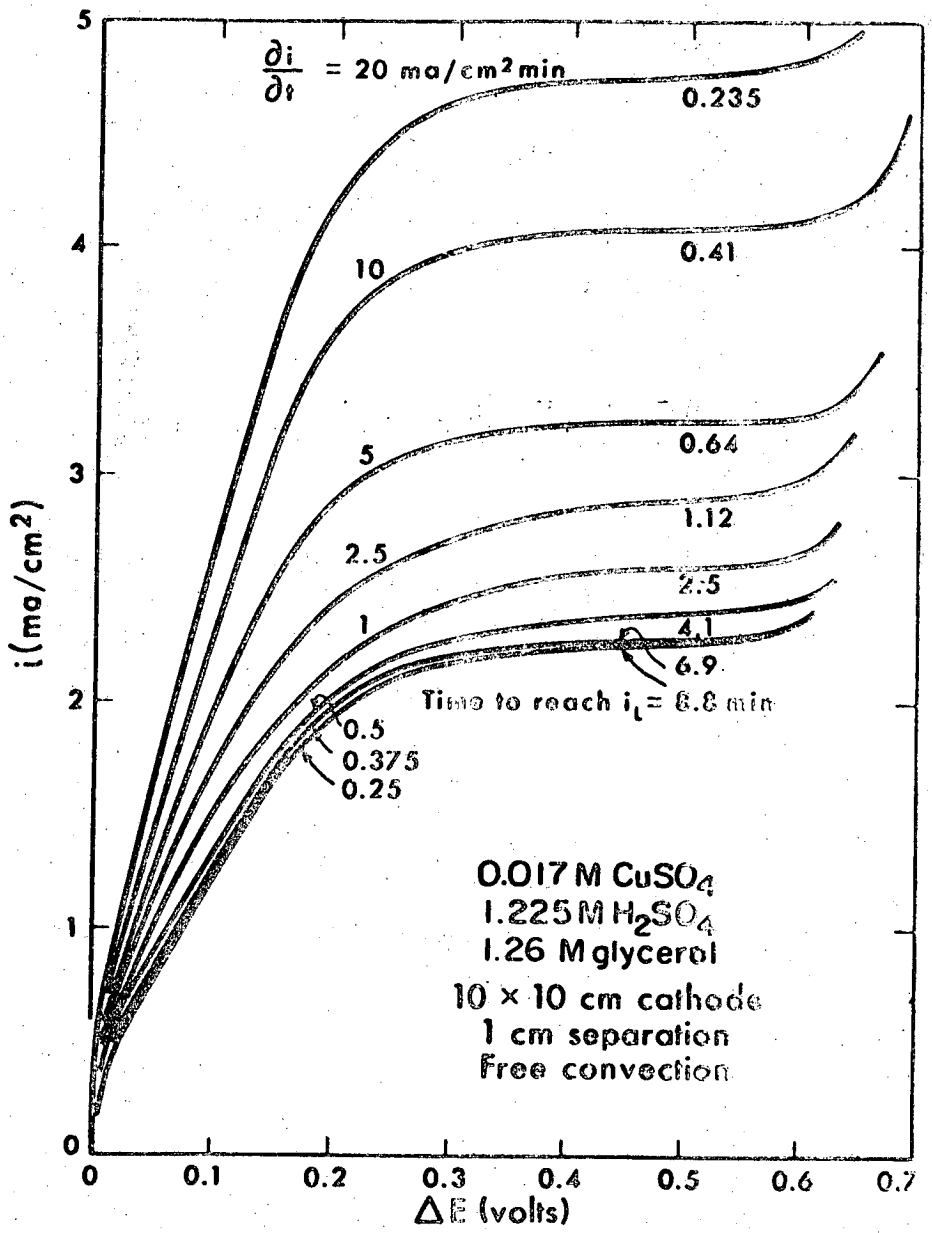

XBL 698-1210 A

Figure 2

Selman - Tobias

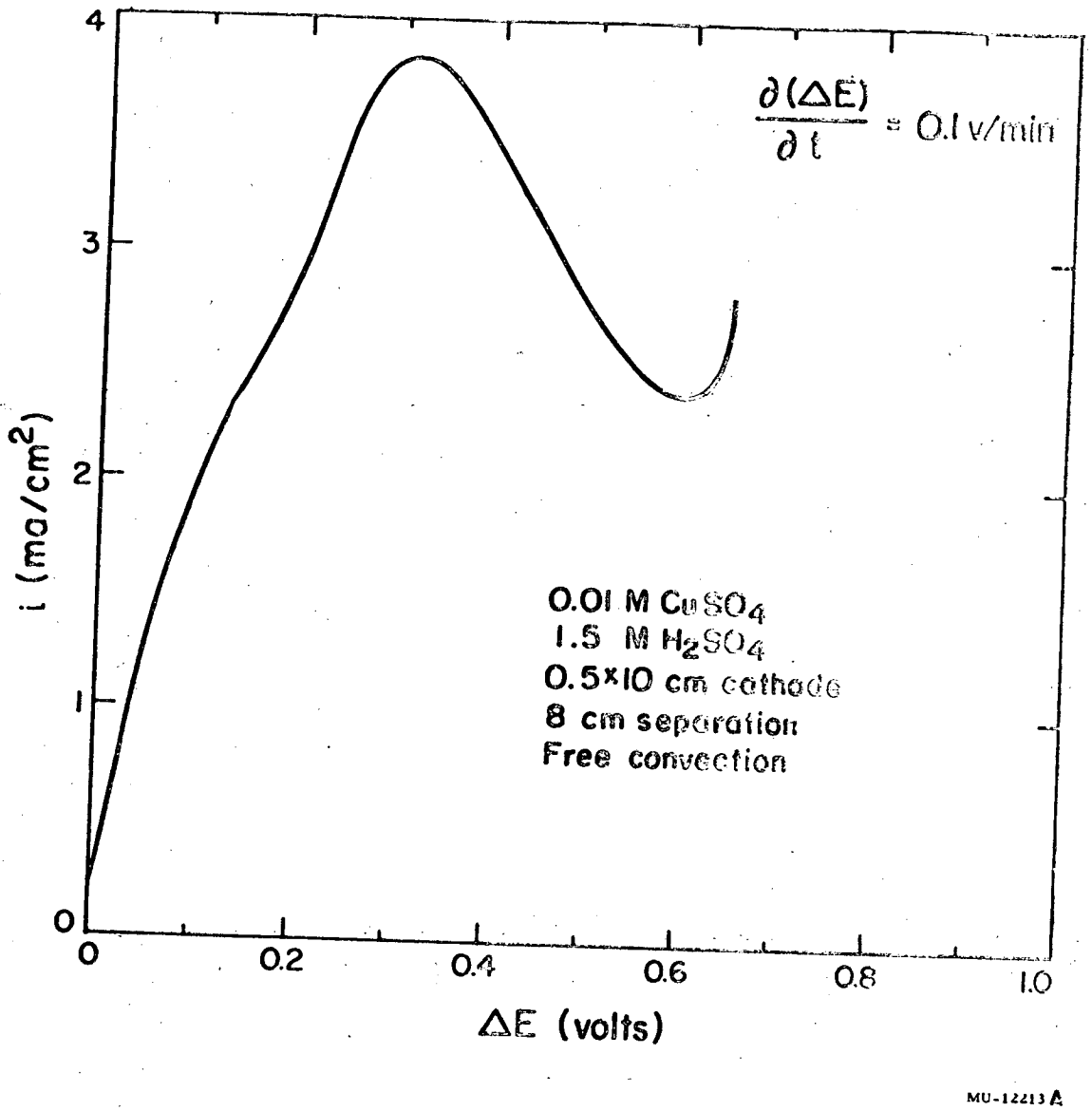

Figure 3

Selman -- Tobias

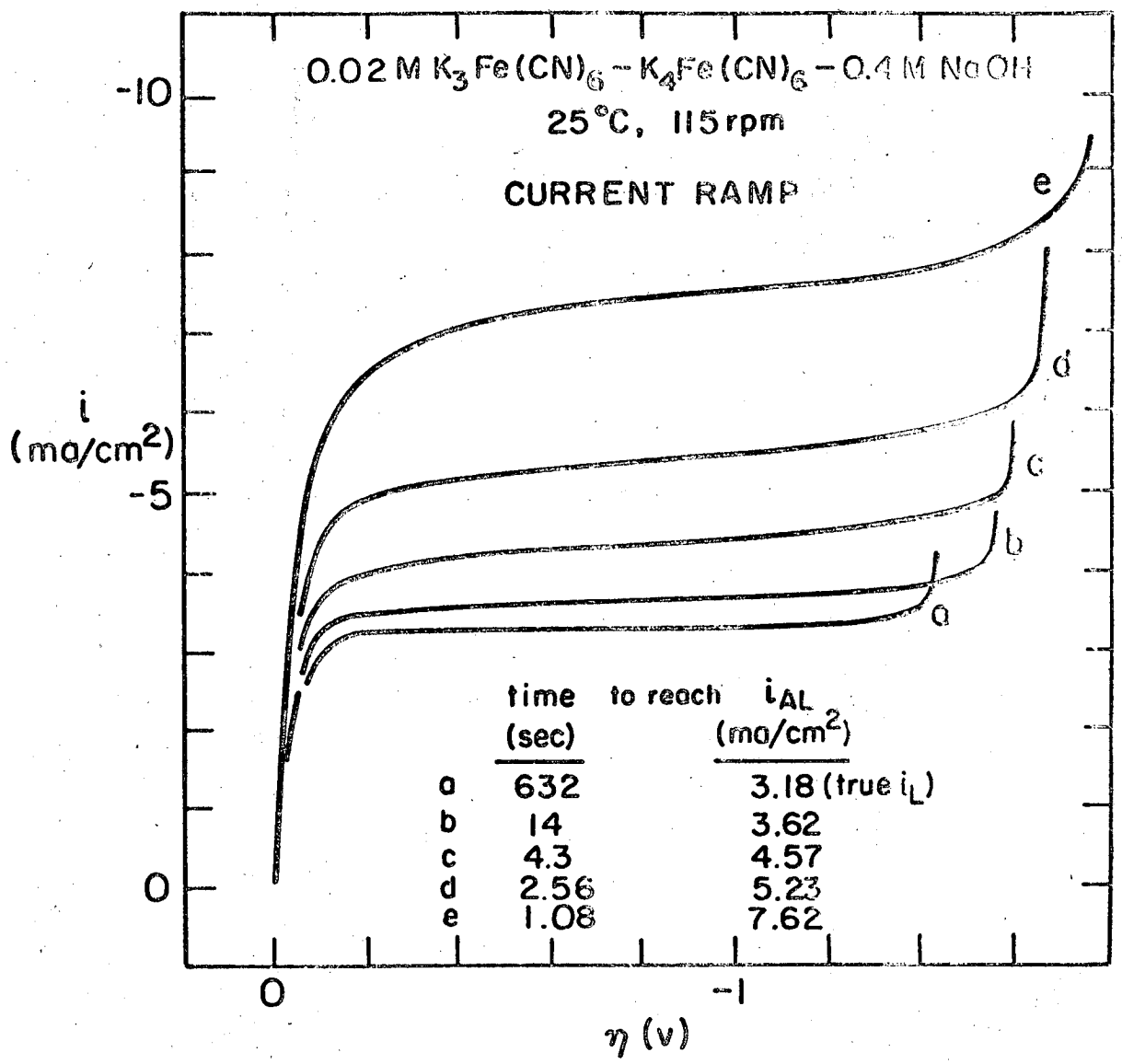

XBL 756-6517

Figure 4

Selman - Tobias

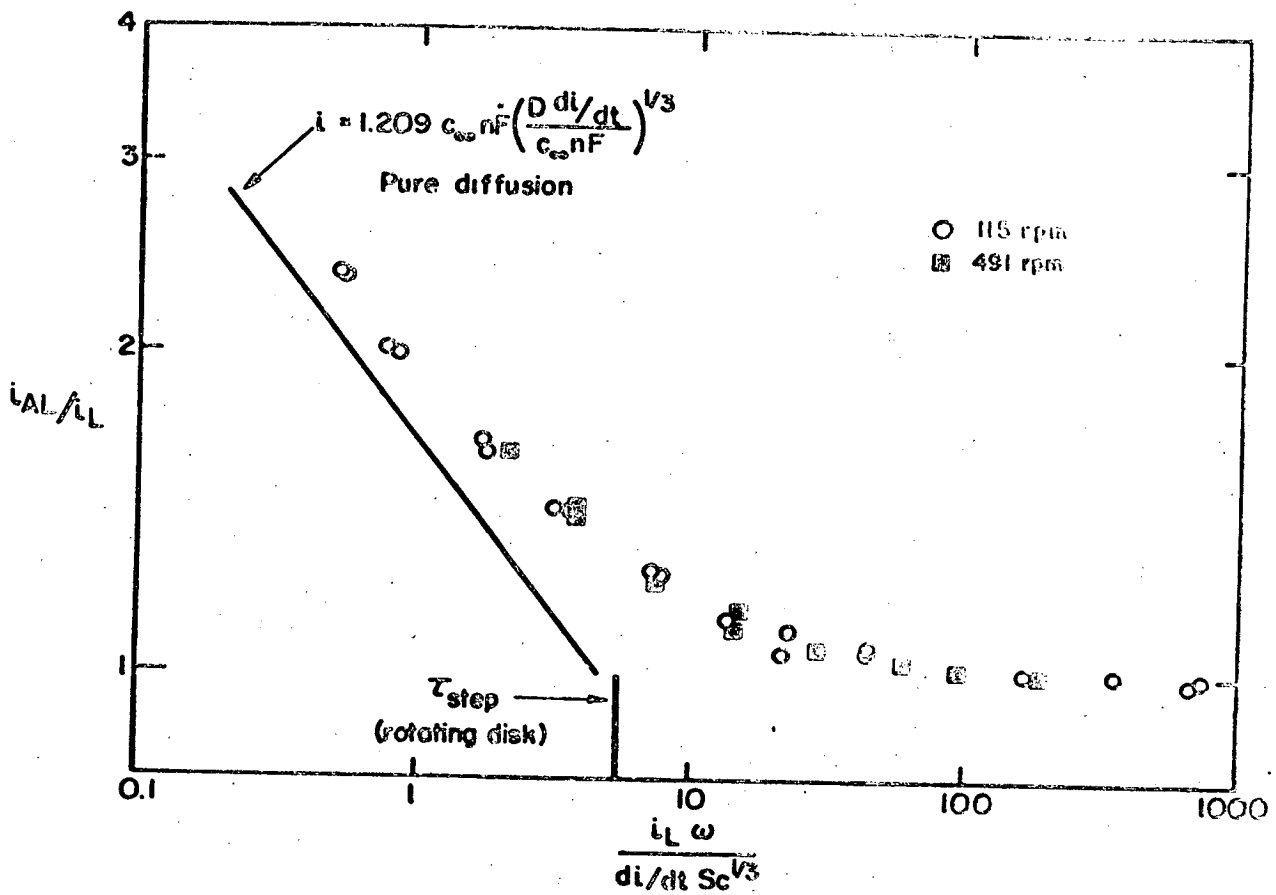

XBL 716-6795

Figure 5

Selman -- Tobias

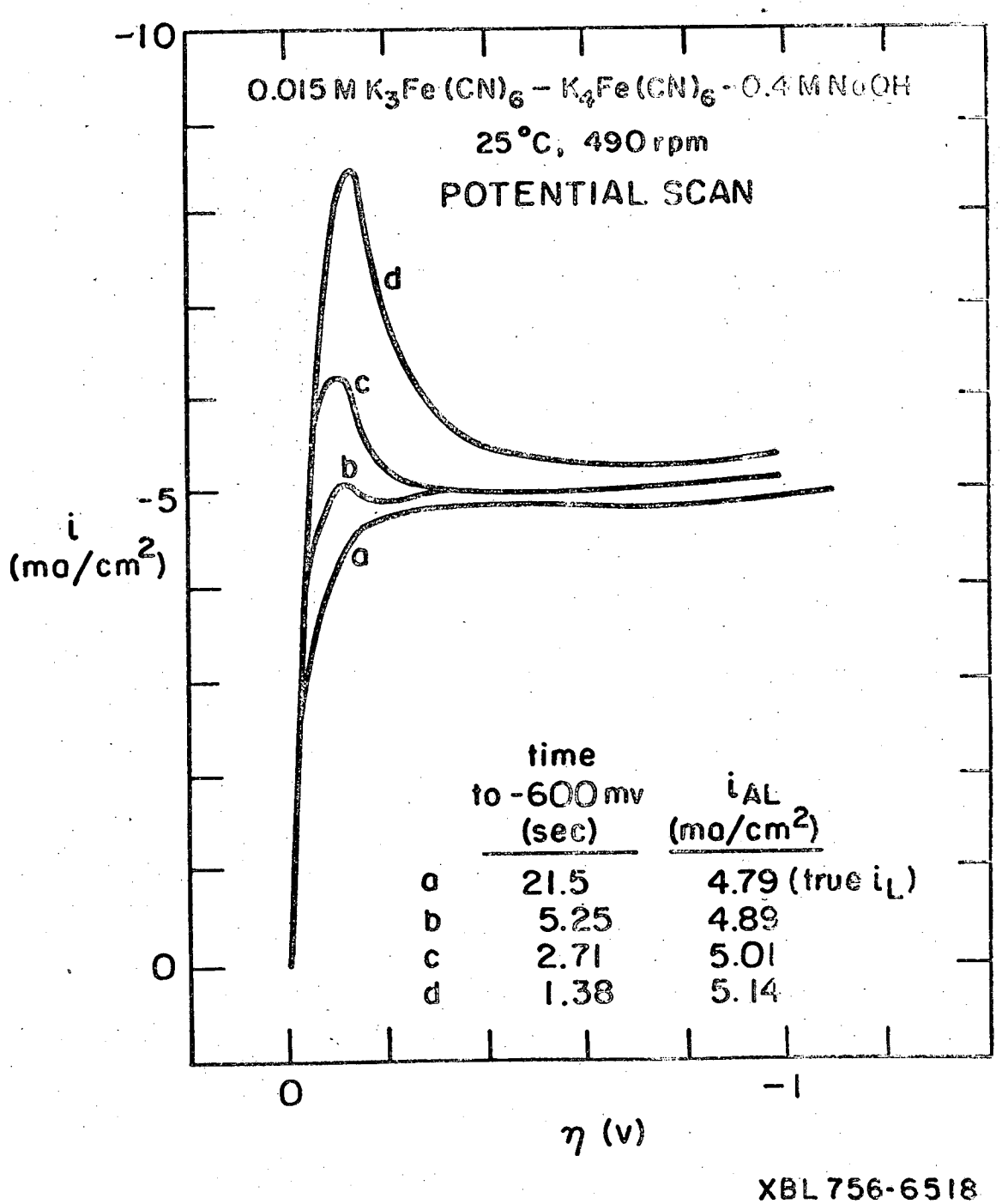

Figure 6

Selman - Tobias

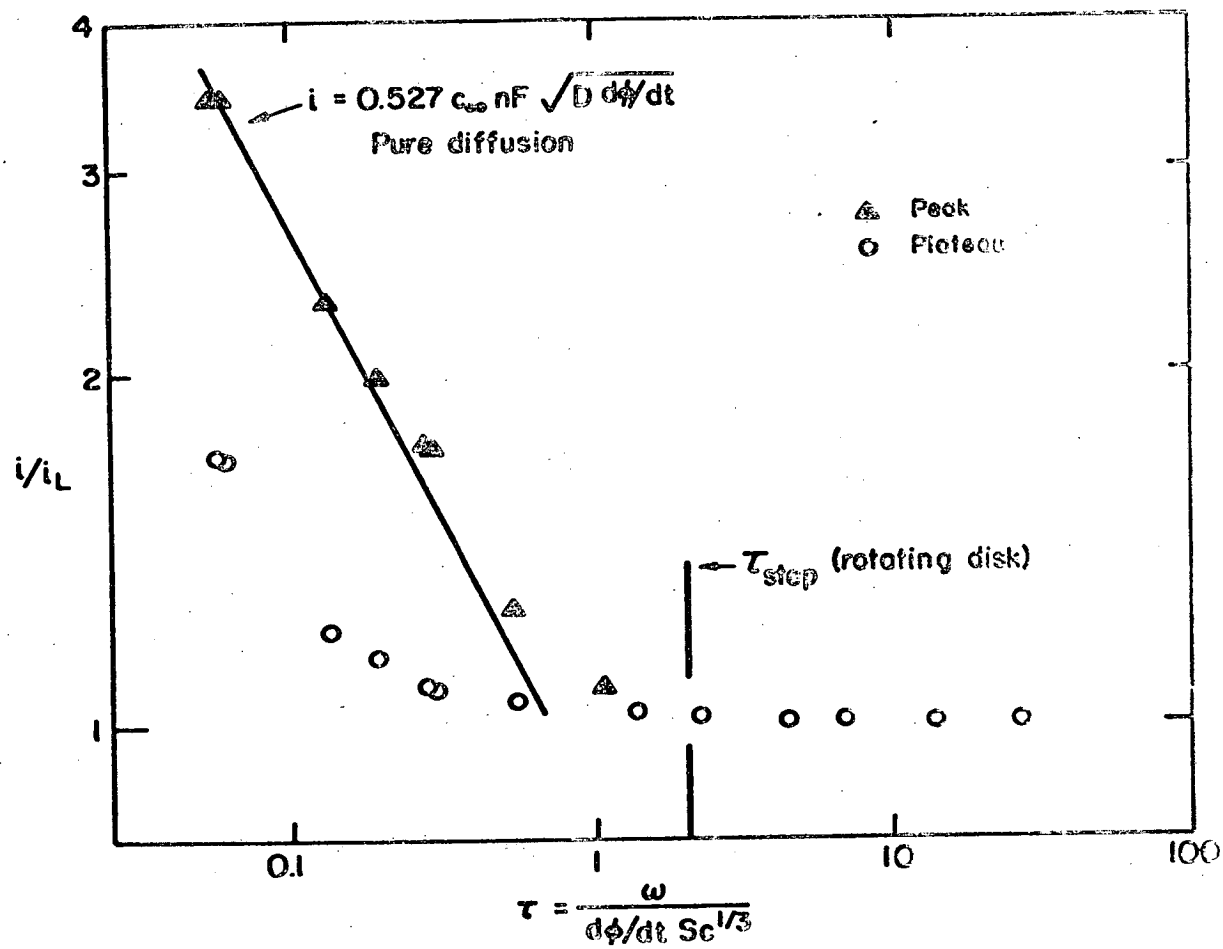

XBL 716-6796

Figure 7

Selman - Tobias

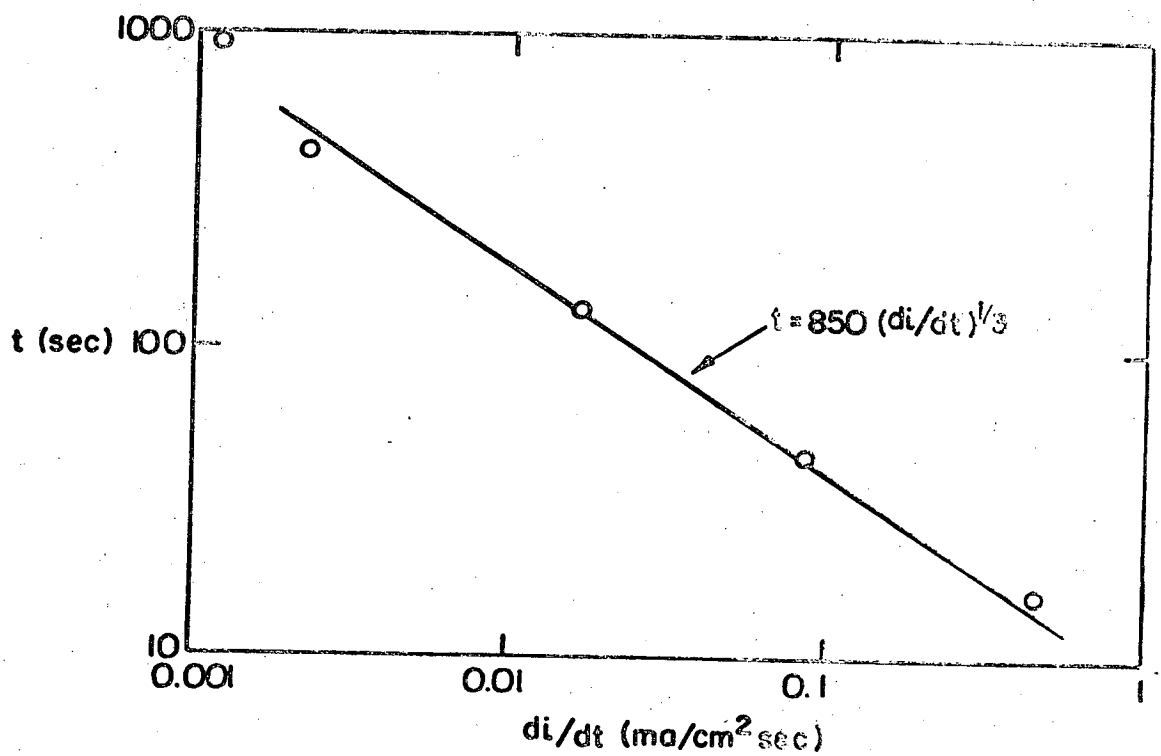

XBL 716-6797

Figure 8

Selman - Tobias

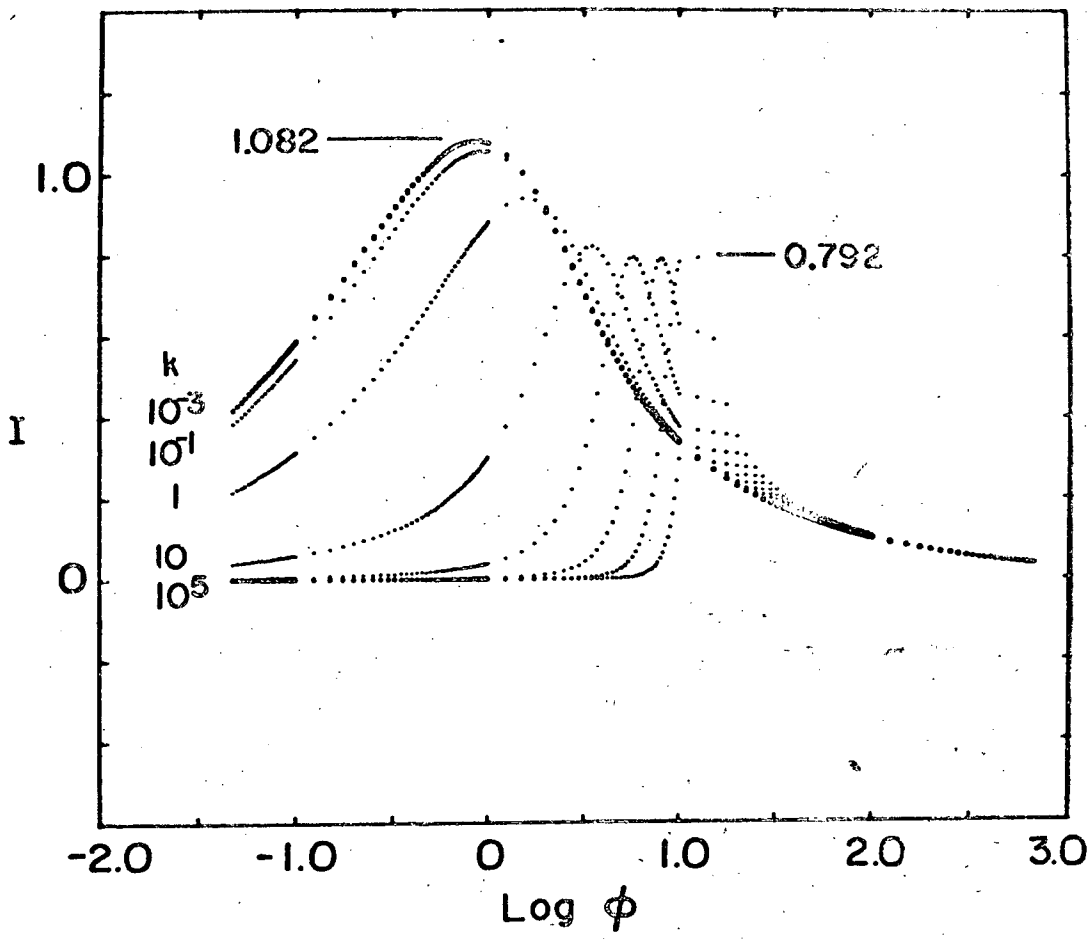

XBL702-2384A

Figure 9

Selman - Tobias

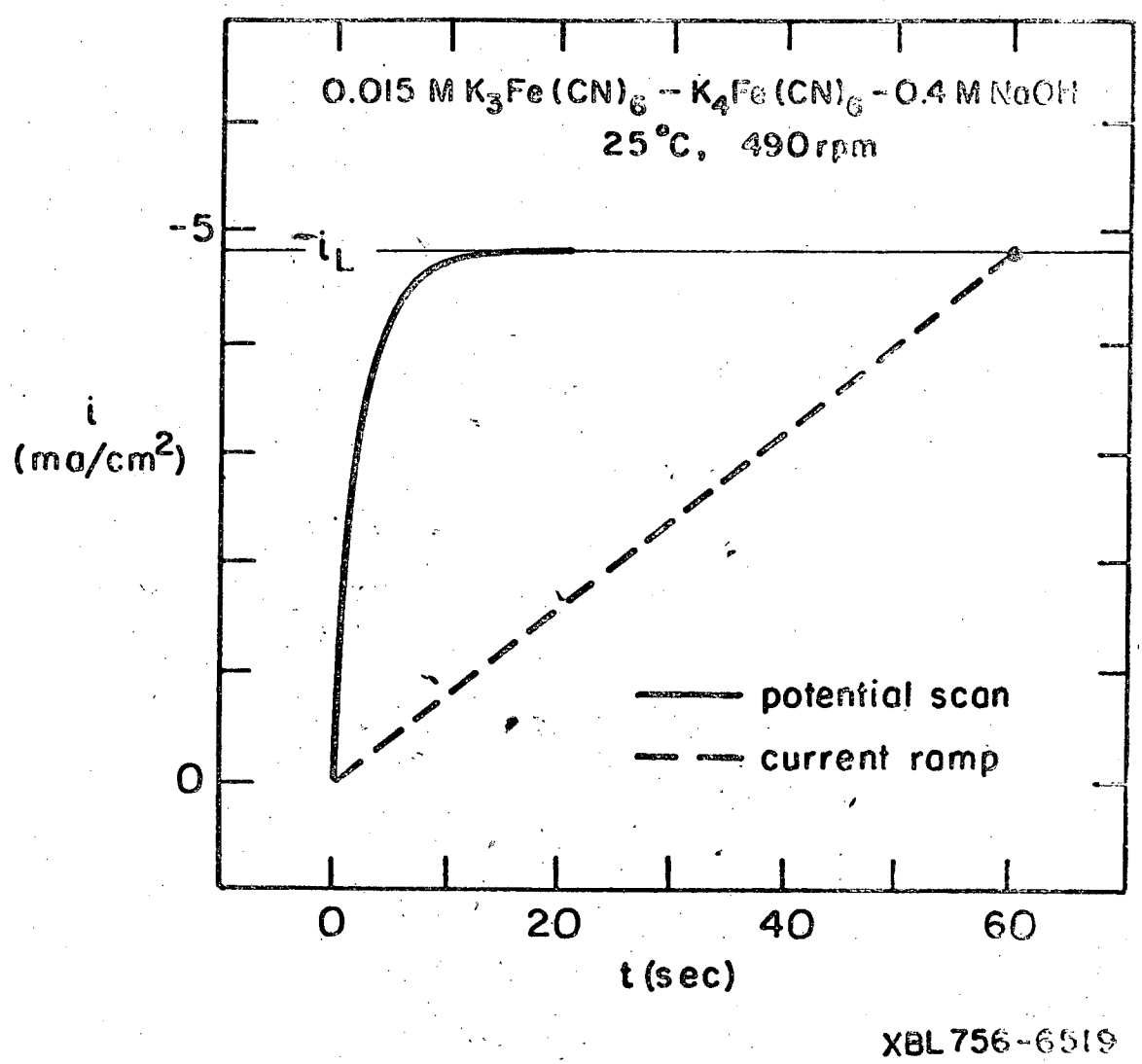

Figure 10

Selman - Tobias

LEGAL NOTICE

This report was prepared as an account of work sponsored by the United States Government. Neither the United States nor the United States Energy Research and Development Administration, nor any of their employees, nor any of their contractors, subcontractors, or their employees, makes any warranty, express or implied, or assumes any legal liability or responsibility for the accuracy, completeness or usefulness of any information, apparatus, product or process disclosed, or represents that its use would not infringe privately owned rights.

TECHNICAL INFORMATION DIVISION
LAWRENCE BERKELEY LABORATORY
UNIVERSITY OF CALIFORNIA
BERKELEY, CALIFORNIA 94720